

Accepted Article

Title: Electron Deficient Monomers Optimizes Nucleation and Enhances Photocatalytic Redox Activity of Carbon Nitrides

Authors: Guigang Zhang, Minghui Liu, Tobias Heil, Spiros Zafeiratos, Aleksandr Savateev, Markus Antonietti, and Xinchun Wang

This manuscript has been accepted after peer review and appears as an Accepted Article online prior to editing, proofing, and formal publication of the final Version of Record (VoR). This work is currently citable by using the Digital Object Identifier (DOI) given below. The VoR will be published online in Early View as soon as possible and may be different to this Accepted Article as a result of editing. Readers should obtain the VoR from the journal website shown below when it is published to ensure accuracy of information. The authors are responsible for the content of this Accepted Article.

To be cited as: *Angew. Chem. Int. Ed.* 10.1002/anie.201908322
Angew. Chem. 10.1002/ange.201908322

Link to VoR: <http://dx.doi.org/10.1002/anie.201908322>
<http://dx.doi.org/10.1002/ange.201908322>

Electron Deficient Monomers Optimizes Nucleation and Enhances Photocatalytic Redox Activity of Carbon Nitrides

Guigang Zhang,* Minghui Liu, Tobias Heil, Spiros Zafeiratos, Aleksandr Savateev, Markus Antonietti and Xinchun Wang*

Abstract: Polymeric carbon nitride (PCN) is usually synthesized from nitrogen-rich monomers such as cyanamide, melamine and urea, but is rather disordered in many cases. Here, a new allotrope of carbon nitride with internal heterostructures was obtained by co-condensation of very electron poor monomers (e.g., 5-amino-tetrazole and nucleobases) in the presence of mild molten salts (e.g., NaCl/KCl) to mediate the polymerization kinetics and thus modulate the local structure, charge carrier properties, and most importantly the HOMO and LUMO levels. Results reveal that the as-prepared NaK-PHI-A material shows excellent photo-redox activities because of a nanometric hetero-structure which enhances visible light absorption and promotes charge separation in the different domains.

The direct conversion of solar energy into storable chemical fuel molecule (e.g., H₂) via photocatalytic water splitting has been regarded as a feasible way to decrease the strong dependence on traditional fossil fuels.^[1-3] The key of this technique however is the development of low-cost, stable and highly efficient photocatalysts, which are able to catalyze the desired reactions in an efficient manner. Among all the investigated photocatalysts, polymeric carbon nitride (PCN) has drawn particular interests owing to its inherent advantages including being metal-free, ease of fabrication, chemical and thermal robustness, and visible light activity.^[4-9] However, direct photocatalytic splitting of water by PCN is rather challenging because PCN in its pristine form features only moderate water oxidation activity.^[10-12]

In principle, PCN is usually prepared by thermal polymerization of carbon and nitrogen containing monomers (e.g., cyanamide, melamine, urea, and many more) at elevated temperatures (usually 550 °C).^[13-15] The polymerization process is at later stages hindered by the sluggish deamination kinetics and thus generates PCN with incomplete condensation and lower local order; it is however potentially still strongly oxidizing (VB=1.82 V, vs. RHE). The created overpotential is however not enough for cocatalyst-free water oxidation, which is -in spite of its apparent simplicity- a remarkably complicated process. PCN however oxidizes many organic compounds, as described in

some recent reviews.^[16-17] Recent progress from our group and other groups reveal that the use of suitable molten salts to mediate the polymerization significantly decreases the number of defects and improves the photo-catalytic performance.^[16-21] Molten salts (e.g., LiCl/KCl, NaCl/KCl) dissolve monomers and intermediates and give a liquid medium for polycondensation, thus improving the local order. Salt melt synthesis provides further the opportunity to synthesize carbon nitride as new allotropes and iso-forms, many coming with higher oxidation potential. Recently, we were able to show that a more “noble” carbon nitride with highly crystalline structure could be obtained when electron deficient triazole/tetrazole based monomers were polycondensed in the LiCl/KCl salt melts.^[22-25] The as-prepared polymers bear much better oxidation activity thanks to the positively shifted HOMO (VB=2.5 V, vs. RHE). However, here the simultaneous downshift of the LUMO (CB=-0.1 V, vs. RHE) results in a weakening of the photocatalytic reduction activity.^[24] Interestingly, excellent reduction ability rather than oxidation activity could be obtained when the tetrazole was polymerized in an alternative NaCl/KCl salt melt.^[26] It is thus exciting to search rationally for other and even more active carbon nitrides, namely more stable conjugated system with both strong oxidation power and good reduction ability for photocatalytic redox reactions, and here we use copolymerization with more electron deficient monomers in diverse molten salts which will turn out to nucleate different allotropes.

The systems are synthesized by copolymerization of electron deficient aminotetrazole in NaCl/KCl molten salts, while we use nucleobases as natural comonomers to introduce local D-A junctions in spurious amounts (~0.3 wt. %). Interestingly, already that little comonomer obviously changes the local electron density, optical absorption, charge carrier transfer process and photocatalytic performance of the as-prepared heptazine based carbon nitrides.

More information about the materials synthesis is found in experimental section (supporting information). In brief, the melon-based carbon nitrides as references were synthesized by thermal polymerization of the monomers dicyandiamide, melamine and urea (denoted as CND, CNM, and CNU). NaK-PHI-based carbon nitrides were obtained by copolymerization of 5-amino-tetrazole (1) without or with nucleobases (2-5) in salt melts (denoted as NaK-PHI, NaK-PHI-A, NaK-PHI-G, NaK-PHI-T, and NaK-PHI-C, respectively).

The as-synthesized poly(heptazine imide) (PHI)-based carbon nitrides were firstly characterized by XRD, FT-IR, and XPS. As seen from Figure S1, such carbon nitrides show only one diffraction peak located 27.4°, corresponding to the graphitic layer stacking distance of the units.^[26-28] The lack of the typical peak at 13°, which is related to the periodic in plane repeat of heptazine units, and the broad diffraction peaks of PHI-based already indicate a local rearrangement of the packing units, which will get more clear in the TEM images later. FT-IR (Figure S2) of the samples reveals that both sample sets of carbon nitrides present similar breathing and stretching modes of the

Dr. G. Zhang, Dr. T. Heil, Dr. A. Savateev, Prof. M. Antonietti
Department of Colloids Chemistry
Max Planck Institute of Colloids and Interfaces
14476 Potsdam (Germany)

E-mail: guigang.zhang@mpikg.mpg.de
M. Liu, Prof. X. Wang

State Key Laboratory of Photocatalysis on Energy and Environment,
College of Chemistry, Fuzhou University
Email:xcwang@fzu.edu.cn

Fuzhou, 350116 (China)

Dr. S. Zafeiratos

ICPEES, Institut de Chimie et des Procédés pour l'Énergie,
l'Environnement et la Santé, UMR 7515 CNRS
Université de Strasbourg 25 rue Becquerel
67087 Strasbourg cedex (France)

Supporting information for this article is given via a link at the end of the document.

heptazine units at 700-850 cm^{-1} and 1200-1600 cm^{-1} , respectively. For the PHI-based carbon nitrides, evident variations at 987 cm^{-1} and 1065 cm^{-1} are observed, revealing the formation of the symmetric and asymmetric variations of imide bound metal ions (here Na/K-NC₂ groups).^[22, 24, 29] The weak absorption band of surface uncondensed amino groups at 3300-3500 cm^{-1} and the strong variations of surface cyano groups at 2177 cm^{-1} reveal the higher extension of polycondensation in the presence of molten salts in comparison with the reference without salts.^[4, 19, 22] Raman spectra were conducted, but both melon and NaK-PHI-A show quite similar triazine/heptazine structures (Figure S3).

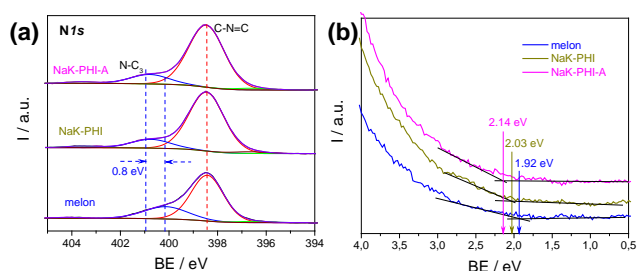


Figure 1. (a) High resolution N1s XPS analysis and (b) UPS analysis of melon, NaK-PHI and NaK-PHI-A.

XPS analysis provides more structural details of the materials. Survey spectra (Figure S4) of the materials show that melon comprises C, N, and O, while PHI-based carbon nitrides are composed with C, N, O, Na and K. High resolution N 1s analysis of the sample shows a clearly positive shift of the N-C₃ species, indicating the stronger electron binding of a more stable and extended conjugation of the PHI-based carbon nitrides, the first indication of a more positive work function of the material.^[30, 31] The successful generation of carbon nitrides with enhanced “nobility” can be also proven by the positive shift of the valence band positions, moving from 1.92 eV of melon to 2.14 eV of NaK-PHI-A, as shown in UPS analysis (Figure 1b). This number, in comparison with the previous reported values of PHI-K, is less positive, but it keeps the strength for a successful photocatalytic water reduction reaction, as certified by the slightly downshift in LUMO (from -1.4 V of melon to -1.22 V of NaK-PHI-A, Mott-Schottky plots of the materials are presented in Figure S5).

The secret of this new structure nucleated from nucleobases is revealed in AC-HRTEM, where we can observe domains with distinct locally ordered structure, different from the weakly ordered structure of melon (Figure S6). The lamellar repeat period is unusually high (ca. 1.65 nm, d_1+d_2), which is of the order of two heptazine units, i.e. we see a periodic superstructure, with the electron contrast presumably created by the charge distribution within a D-A-structure. In some selected parts of the picture, we even can see that the 1.65 nm repeat is breaking up into two layer distances of ca. 0.67 nm and ca. 0.98 nm, (Figure 2a). The formation of new stacking distance of 0.67 nm (smaller than the traditional packing distance of about 0.92 nm in unmodified PHI) can indicate a tilted stacking between neighboring heptazine units (tilt angle then around 40 °), very

similar to J-aggregates of dye molecules. As J-aggregated usually allows a red shift of the absorption band and higher thermodynamic stability, while H-packing then correspond to the usual PHI-packing, we would have a simple observation of the observed electronic and contrast features. Electron-hole separation would then simply occur between the different stacks, thus greatly simplifying local charge separation and charge transport in each well aligned molecular columns (see local D-A junction as depicted in Scheme S2). We also find new optical absorption transitions beyond the intrinsic π - π^* electron transitions of the standard heptazine stacks. The role of 0.3% nucleobases in this structure is still unclear to us and deserved further analysis, but we have to assume that primary condensation structures are able to nucleate such bipolar stacks, which then simply continue to grow, i.e. it is the classical role of a nucleation agent.^[32, 33]

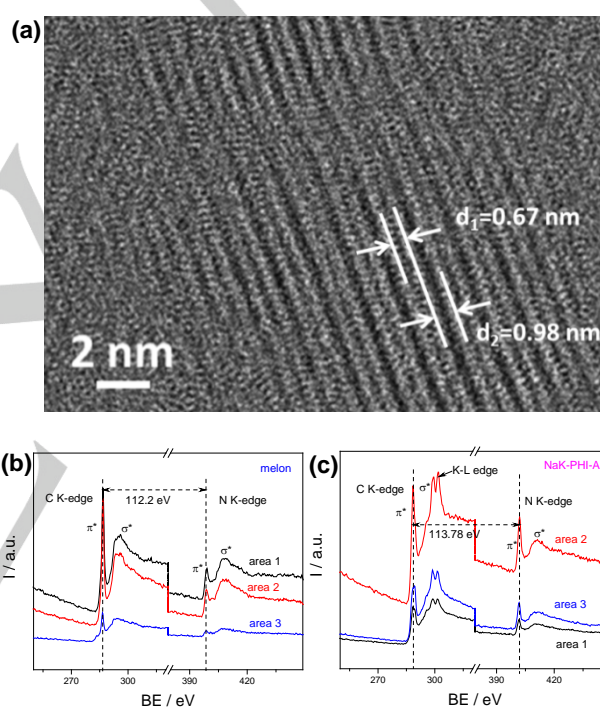


Figure 2. (a) Fourier filtered HR-TEM image of the selected area of NaK-PHI-A; C-K edge and N-K edge EELS of (b) melon and (c) NaK-PHI-A.

Interestingly, relevant electronic details of the materials could be revealed by the C-K and N-K edges EELS of the samples (Figure 2 b and c). It is clearly to observe that both samples exhibit a typical carbon nitride structure comprising of both π^* and σ^* -transitions, while however the σ^* -transition of carbon is much sharper in the new material than that of melon, which potentially can be related to the extra C-T band also seen in optical absorption. On top of that, the distance between the carbon and the nitrogen EELS peaks is increased from 112.2 to 113.8 eV, and this positive change in the binding energy (~1.6 eV) is mostly due to stronger binding of electrons also at the nitrogen position, i.e. the overall electronic structure with its positive change in the binding energy indicates a lower valance

band of a more stable polymorph.^[24] This is in very good accordance with the XPS and UPS data discussed above.

Another difference of the new and the reference carbon nitrides is the surface morphology. SEM images of PHI-based carbon nitrides (Figure S7) confirm the re-organization of the crystals in the presence of salt melts. Especially with the guanine containing samples we see in the surface texture well faceted primary crystals of 20-50 nm in size, thus supporting our nucleation hypothesis. These primary particles are however inter-grown to a dense bulk, with planar grain boundaries as depicted in Fig. 2a. BET analysis (Figure S9) of the samples illustrate that the specific surface area of NaK-PHI-A is only $11 \text{ m}^2 \text{ g}^{-1}$, which is slightly larger than that of weakly ordered melon (e.g., CND, $5 \text{ m}^2 \text{ g}^{-1}$) but much lower than that of a porous mpg-CN ($125 \text{ m}^2 \text{ g}^{-1}$) because of the intergrowth of the primary crystals. Besides, SEM elemental mapping (Figure S8) of the NaK-PHI-A sample conform the even distribution of the C, N, Na, and K elements.

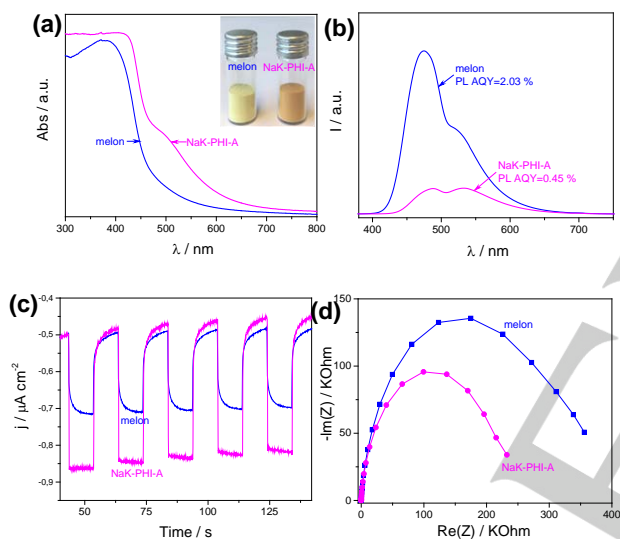


Figure 3. (a) UV-Vis absorption spectra, (b) room temperature steady state Photoluminescence spectra, (c) transient photocurrent under visible light irradiation and (d) electrochemical impedance spectroscopy (EIS) of melon and NaK-PHI-A.

The optimized D-A heterostructured carbon nitrides also show significantly improved optical and electronic properties, when compared to the melon-based counterparts. UV-Vis spectra of both melon and PHI-based carbon nitrides in Figure 3a and Figure S10, but also sheer colour reflect the obvious difference in optical absorption. The new system has a stronger transition moment as a semiconductor, but also an extra CT band partly covering the visible spectrum. The optical band gaps of the reference and the new material are calculated to be 2.65 and 2.51 eV, respectively. This absorption, when attributed to a sigma- Pi star transition, is forbidden for perfectly symmetric and planar units,^[32-34] but might be activated by the creation of the new packing mode as described in HR-TEM. Another option is the direct optical excitation of a D-A transition. Figure 3b depicts the room-temperature photoluminescence (PL) spectra of the materials. It is easy to observe that NaK-PHI-A possesses much

lower PL emission intensity than melon, indicating suppressed recombination of the radioactive charge carrier.^[7, 8, 35] Time resolved PL (Figure S11) reveal that the mean radioactive lifetimes ($\Delta\tau$) of the recombining charge carriers of melon and NaK-PHI-A were calculated to be 12.18 and 3.88 ns, respectively. It is most likely the local heterostructure in the crystalline polymer accelerates the charge transfer over the interface.^[36] The better charge carrier transfer can also be revealed by transient photocurrent generation and the electrochemical impedance spectroscopy (Figure 3c and d). A steady and clearly enhanced photocurrent was generated for the NaK-PHI-A. Meanwhile, the smaller EIS radius of the NaK-PHI-A electrode than that of melon also suggests a faster charge carrier transfer, which is beneficial to improve the photocatalytic performance.^[37]

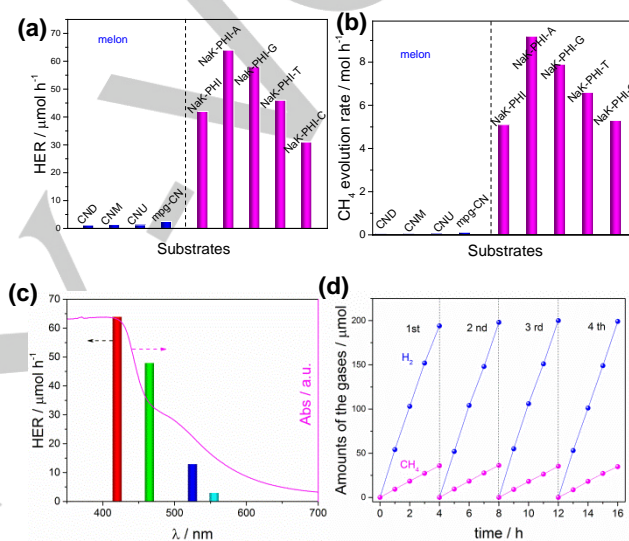


Figure 4. Photocatalytic activities of melon and PHI-based carbon nitrides under visible light irradiation for (a) H_2 production and (b) CH_4 production, (c) wavelength-dependent H_2 evolution of from water and ethanol mixture and (d) time course H_2 and CH_4 production catalyzed by optimized NaK-PHI-A.

The photocatalytic performance of the as-prepared melon and PHI-based samples was then firstly evaluated by H_2 production from water in the presence of Pt as cocatalysts and triethanolamine (TEOA) as a sacrificial agent for oxidation. As shown in Figure S11, all the PHI-based carbon nitrides exhibit much better performances ($178\text{-}342 \mu\text{mol h}^{-1}$) than the melon-based counterparts, even much better than the mpg-CN ($94 \mu\text{mol h}^{-1}$) with large surface area, indicating overall better photochemistry for the complete reaction chain. As specific BET surface area of NaK-PHI-based carbon nitrides is only $\sim 11 \text{ m}^2 \text{ g}^{-1}$, much lower than that of mpg-CN ($125 \text{ m}^2 \text{ g}^{-1}$), this improvement is even more remarkable for a heterogeneous photocatalyst.

Besides, the PHI-based carbon nitrides also show excellent performance for photocatalytic H_2 production by reforming of another, more critical sacrificial agent, i.e. ethanol. From Figure 4a we can see that all melon-based carbon nitrides are inactive for photocatalytic oxidation of ethanol, as evidenced by slow H_2 production (lower than $5 \mu\text{mol h}^{-1}$). In contrast, all PHI-based

carbon nitrides present evidently enhanced activity (~12 times faster) for the photocatalytic reforming of ethanol (HER=31-64 $\mu\text{mol h}^{-1}$). This clearly points to improved oxidation strength, as targeted by the molecular design, while the capabilities for reduction are obviously not compromised.

The improved photoredox performance of the D-A heterojunction carbon nitrides can be also proven by a new reaction, the disproportionation of ethanol into CO_2 and CH_4 (see mechanism in Scheme S3 and GC-MS analysis of the products in Figure S12). In Figure 4b we can see that all PHI-based carbon nitrides show high CH_4 evolution, while melon-based carbon nitrides are only slightly active. The formation of a local, excited D-A heterojunction obviously facilitates both photo-oxidation and photoreduction, on separate site of the crystals. The optimum NaK-PHI-A shows an apparent quantum efficiency of ~9.6 % for photocatalytic reforming of ethanol, which is better than most of the previous reported polymeric photocatalysts under the same conditions (see comparisons in Table S1).

Some secondary benefits lie for instance in the fact that the optimized Pt loading contents (0.3 wt. %, Figure S13) is much lower than that of 3 wt. %, when using TEOA as an oxidation sacrificial agent, speaking of course for better charge transport to localized active sites. In addition, the new D-A- material is active even at irradiation wavelengths of 555 nm (Figure 4c), indicating that also this transition creates effectively light-induced charge pairs that can be readily used for photochemistry. In addition, the new material shows very good stability in long time photocatalytic reactions (Figure 4d). After 4 runs, almost no lowering of gas evolution was found, illustrating robustness against light and solution corrosion. No structure change of the material is found even after long time reaction (Figure S14-16), indicating the robust stability against light and solution corrosion.^[38]

In conclusion, a series of PHI-based carbon nitrides were obtained by condensation of 5-amino-tetrazole in the presence of minor amounts of nucleobases. The results reveal that these materials bear an inter-columnar superstructure with different stacking motifs that can act as a D-A heterojunction. This local effect leads to enhanced optical absorption, more stable conjugated systems and improved electronic properties, which speed up the charge transfer and promote the photocatalytic activity, such as exemplifies with H_2 and CH_4 production assays. This study provides a promising way to structure photocatalytic redox active polymers by nucleation effects in a mild salt melt to modulate the local structure and charge transfer processes.

Acknowledgements

G. Z. thanks the Alexander von Humboldt Foundation for a postdoctoral fellowship. This work is financially supported by the Max Planck Institute of Colloids and Interfaces and the National Natural Science Foundation of China (21761132002 and 21425309), the National Key R&D Program of China (2018YFA0209301), and the 111 Project (D16008).

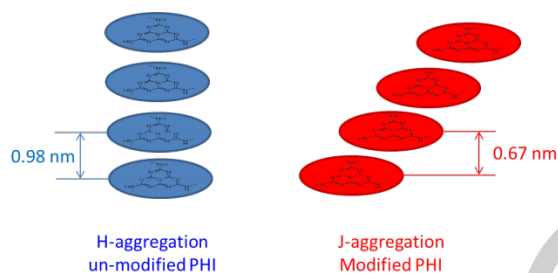
Keywords: packing geometry • electron deficient monomers • carbon nitride • water splitting • photocatalysis

- [1] N. S. Lewis, D. G. Nocera, *Proc. Natl. Acad. Sci. U. S. A.* **2006**, *103*, 15729-15735.
- [2] A. Listorti, J. Durrant, J. Barber, *Nat. Mater.* **2009**, *8*, 929-930.
- [3] K. Maeda, M. Higashi, D. Lu, R. Abe, K. Domen, *J. Am. Chem. Soc.* **2010**, *132*, 5858-5868.
- [4] G. Zhang, L. Lin, G. Li, Y. Zhang, A. Savateev, X. Wang, M. Antonietti, *Angew. Chem. Int. Ed.* **2018**, *57*, 9372-9376.
- [5] W. J. Ong, L. L. Tan, Y. H. Ng, S. T. Yong, S. P. Chai, *Chem. Rev.* **2016**, *116*, 7159-7329.
- [6] D. J. Martin, P. J. T. Reardon, S. J. A. Moniz, J. Tang, *J. Am. Chem. Soc.* **2014**, *136*, 12568-12571.
- [7] W. J. Ong, L. L. Tan, S. P. Chai, S. T. Yong, *Chem. Commun.* **2015**, *51*, 858-861.
- [8] H. Wang, X. Sun, D. Li, X. Zhang, S. Chen, W. Shao, Y. Tian, Y. Xie, *J. Am. Chem. Soc.* **2017**, *139*, 2468-2473.
- [9] K. Schwinghammer, M. B. Mesch, V. Duppel, C. Ziegler, J. Senker, B. V. Lotsch, *J. Am. Chem. Soc.* **2014**, *136*, 1730-1733.
- [10] G. Zhang, Z. Lan, L. Lin, S. Lin, X. Wang, *Chem. Sci.* **2016**, *7*, 3062-3066.
- [11] G. Zhang, S. Zang, X. Wang, *ACS Catal.* **2015**, *5*, 941-947.
- [12] M. Zhu, S. Kim, L. Mao, M. Fujitsuka, J. Zhang, X. Wang, T. Majima, *J. Am. Chem. Soc.* **2017**, *139*, 13234-13242.
- [13] M. Shalom, S. Inal, C. Fettkenhauer, D. Neher, M. Antonietti, *J. Am. Chem. Soc.* **2013**, *135*, 7118-7121.
- [14] J. Zhang, G. Zhang, X. Chen, S. Lin, L. Möhlmann, G. Dolega, G. Lipner, M. Antonietti, S. Blechert, X. Wang, *Angew. Chem. Int. Ed.* **2012**, *51*, 3183-3187.
- [15] S. Guo, Z. Deng, M. Li, B. Jiang, C. Tian, Q. Pan, H. Fu, *Angew. Chem. Int. Ed.* **2016**, *55*, 1830-1834.
- [16] A. Savateev, M. Antonietti, *ACS Catal.* **2018**, *8*, 9790-9808.
- [17] A. Savateev, I. Ghosh, B. König, M. Antonietti, *Angew. Chem. Int. Ed.* **2018**, *57*, 15936-15947.
- [18] M. K. Bhunia, K. Yamauchi, K. Takanabe, *Angew. Chem. Int. Ed.* **2014**, *53*, 11001-11005.
- [19] M. J. Bojdy, J. O. Müller, M. Antonietti, A. Thomas, *Chem. Eur. J.* **2008**, *14*, 8177-8182.
- [20] K. Schwinghammer, B. Tuffy, M. B. Mesch, E. Wirnhier, C. Martineau, F. Tauelle, W. Schnick, J. Senker, B. V. Lotsch, *Angew. Chem. Int. Ed.* **2013**, *52*, 2435-2439.
- [21] G. Zhang, G. Li, Z. Lan, L. Lin, A. Savateev, T. Heil, S. Zafeiratos, X. Wang, M. Antonietti, *Angew. Chem. Int. Ed.* **2017**, *56*, 13445-13449.
- [22] Y. Ham, K. Maeda, D. Cha, K. Takanabe, K. Domen, *Chem. Asian J.* **2013**, *8*, 218-224.
- [23] L. Lin, H. Ou, Y. Zhang, X. Wang, *ACS Catal.* **2016**, *6*, 3921-3931.
- [24] A. Savateev, S. Pronkin, J. D. Epping, M. G. Willinger, C. Wolff, D. Neher, M. Antonietti, D. Dontsova, *ChemCatChem* **2017**, *9*, 167-174.
- [25] D. Dontsova, S. Pronkin, M. Wehle, Z. Chen, C. Fettkenhauer, G. Clavel, M. Antonietti, *Chem. Mater.* **2015**, *27*, 5170-5179.
- [26] G. Zhang, G. Li, T. Heil, S. Zafeiratos, F. Lai, A. Savateev, M. Antonietti, X. Wang, *Angew. Chem. Int. Ed.* **2019**, *58*, 3433-3437.
- [27] I. Y. Kim, S. Kim, X. Jin, S. Premkumar, G. Chandra, N. Lee, G. P. Mane, S. Hwang, S. Umapathy, A. Vinu, *Angew. Chem. Int. Ed.* **2018**, *57*, 17135-17140.
- [28] G. Zhang, M. Zhang, X. Ye, X. Qiu, S. Lin, X. Wang, *Adv. Mater.* **2014**, *26*, 805-809.
- [29] Y. Guo, J. Li, Y. Yuan, L. Li, M. Zhang, C. Zhou, Z. Lin, *Angew. Chem. Int. Ed.* **2016**, *55*, 14693-14697.
- [30] G. Liu, T. Wang, H. Zhang, X. Meng, D. Hao, K. Chang, P. Li, T. Kako, J. Ye, *Angew. Chem. Int. Ed.* **2015**, *54*, 13561-13565.
- [31] D. C. Bradley, M. H. Gittitz, *J. Chem. Soc. A* **1969**, *0*, 980-984.
- [32] Z. Chen, A. Savateev, S. Pronkin, V. Papaefthimiou, C. Wolff, M. G. Willinger, E. Willinger, D. Neher, M. Antonietti, D. Dontsova, *Adv. Mater.* **2017**, *29*, 1700555.
- [33] H. Ou, L. Lin, Y. Zheng, P. Yang, Y. Fang, X. Wang, *Adv. Mater.* **2017**, *29*, 1700008.

- [34] G. Zhang, A. Savateev, Y. Zhao, L. Li, M. Antonietti, *J. Mater. Chem. A* **2017**, *5*, 12723-12728.
- [35] Y. Chen, B. Wang, S. Lin, Y. Zhang, X. Wang, *J. Phys. Chem. C* **2014**, *118*, 29981-29989.
- [36] a) X. Liu, B. Liu, L. Li, Z. Zhuge, P. Chen, C. Li, Y. Gong, L. Niu, J. Liu, L. Lei, C. Q. Sun, *Appl. Catal. B: Environ.* **2019**, *249*, 82-90; b) S. Hou, X. Xu, M. Wang, T. Lu, C. Q. Sun, L. Pan, *Chem. Eng. J.* **2018**, *337*, 398-404.
- [37] B. Liu, X. Liu, J. Liu, C. Feng, Z. Li, C. Li, Y. Gong, L. Pan, S. Xu, C. Q. Sun, *Appl. Catal. B: Environ.* **2018**, *226*, 234-241.
- [38] B. Liu, X. Liu, L. Li, Z. Zhuge, Y. Li, C. Li, Y. Gong, L. Niu, S. Xu, C. Q. Sun, *Appl. Surf. Sci.* **2019**, *484*, 300-306.

COMMUNICATION

Copolymerization with electron deficient monomers in salt melt optimizes the nucleation, local packing mode, band structure and optical properties of carbon nitride polymers.



G. Zhang,* M. Liu, T. Heil, S. Zafeirotos, A. Savateev, M. Antonietti and X. Wang*

Page No. – Page No.

**Electron Deficient Monomers
Optimizes Nucleation and
Enhances Photocatalytic
Redox Activity of Carbon
Nitriles**

Accepted Manuscript